Effects of Thermal Preload Change and Preload Relaxation of Bolted Joints as Base for Positive Long-term Behaviour

Bolted joints are the primary method for joining components and transferring forces, making their long-term reliability critical for product success and lightweight design. However, design calculations often focus on the initial assembly load and elastic preload change as a result of thermal or mechanical loads, neglecting long-time effects due to preload relaxation. This paper presents experimental measurements of the preload relaxation behaviour focussing on primary influence factors like temperature, initial preload, thread engagement and head bearing diameter of steel bolts and clamped components and nuts. A key finding is that during the first heating after tightening plastification occurs, which is the reason for a much smaller preload at operating temperature than calculated. Regular bolts with a smaller head bearing diameter have significantly less preload due to the limiting surface pressure, which can also be seen in surface measurements. Increasing the initial preload doesn't necessarily result in a higher preload over time, because it will result in higher plastification during the first hours of thermal expansion. Decreasing the thread engagement is critical and can lead to severe preload losses. An effective way to counter the preload loss is to retighten the bolted joint connection after the first temperature exposure.

Keywords: *Bolted joints, engineering design, preload relaxation, thermal- and time behaviour, design of component and assembly process*

Introduction to the time- and temperature-dependent behaviour of lightweight bolted joints

Due to the high degree of standardization, extensive design guidelines like the VDI 2230 (VDI 2015 (current edition)) and the advantage of high clamping forces combined with the ability to disassemble the connection, bolted joint connections are widely used in the industry. Applications are exceptionally diverse, ranging from miniature bolts with diameters under Ø1 mm used in smartphone up to large M72 bolts utilized in wind turbines. The systematic design of high-duty bolted joints include parameters like mechanical loads (e.g. static and/or dynamic axial, transverse, eccentric load application, torsion and bending moments), geometry of the connection (resilience, number of joint interfaces, length of thread engagement), materials (e.g. property class of the bolt, yield strength and thermal expansion coefficient), tribology (friction coefficients, coating, surface treatment) and assembly conditions (e.g. torque-, angle- or yield-controlled tightening). The primary design criterion although is the determination and maintenance of a sufficiently high preload force to prevent a failure of the connection like leaking, interface opening, self-loosening or increasing contact resistance in busbars.

Lightweight design concepts are gaining increasing importance across numerous technical fields, including joining technology. The use of lightweight materials like aluminium components combined with high-strength steel bolts facilitate an efficient reduction in structural mass and therefore a reduction on energy consumption of moving parts. On the other hand, it simultaneously increases the requirements on joint design to ensure the functionality over the planned lifetime. While the VDI 2230 guideline gives a good estimation of the behaviour of bolted joint connections at around room temperature and can calculate the elastic preload change due to different thermal expansion coefficients, the preload loss due to the damage mechanism of preload relaxation isn’t covered yet. Particularly for lightweight materials such as aluminium, where creep deformation must be anticipated at temperatures as low as 80 °C (homologous temperature $T/T_m \approx 0{,}4$), this damage mechanism has to be considered in the design process.

Preload relaxation is the result of the superposed mechanisms seating, load plastification and creeping, which can be seen in **Figure 1**. The applied preload for the bolted joint connection ranges from F_{Pmin} to F_{Pmax}, determined by the assembly method. All mechanism of the preload relaxation will lead to plastification which occur after tightening and will lead to a preload loss.

Depending on the surface roughness in the contact areas (between bolt and clamped part, joint intersections, the clamped part and nut and engaged threads) and load type, a time-dependent surface smothering takes places, which will lead to a shortening and therefore to a preload loss in the first 10 hours (Duchard 2013) to 72 hours (Ba-Saleem 1991), which is described as seating. An estimation of the loss due to seating for heavy steel-only bolted joint connections in dependency of the surface roughness, number of joint interfaces and direction of loading can be calculated with the VDI 2230 guideline. Due to the application of an operating temperature an 2nd stage of seating can be observed as a result of a thermal induced preload rise and thermal degradation of material properties. The thermal induced preload depends not only on the combination of materials (e.g. steel bolt with an thermal expansion coefficient of $\alpha_{St} \approx 11 \cdot 10^{-6}\ K^{-1}$ and aluminium part with $\alpha_{Al} \approx 23 \cdot 10^{-6}\ K^{-1}$), but also of the geometry of the connection. An increased clamping length will lead to a bigger elongation of the aluminium part compared to the steel bolt and this results in an increase of preload on the one hand, but on the other hand there will be additional roughness embedment in the contact areas. The higher preload also affects the intensity of the creep simultaneously. As soon as the temperature drops again to room temperature, the embedment can be seen as a preload loss.

Load plastification describes plastification due to irregular mechanical and/or thermal loads, which can also occur because of insufficient material properties or preload levels, which exceed the limiting surface pressure (Arz 2023).

Creeping of materials is a time-, load- and temperature-dependent transformation of elastic to plastic strain which occur in the crystal lattice. In bolted joint connections we usually just have first and second stage creep, as the preload will reduce according to the plastification and third stage won’t be reached.

Figure 1. *Damage mechanism of preload relaxation (Friedrich 2013)*

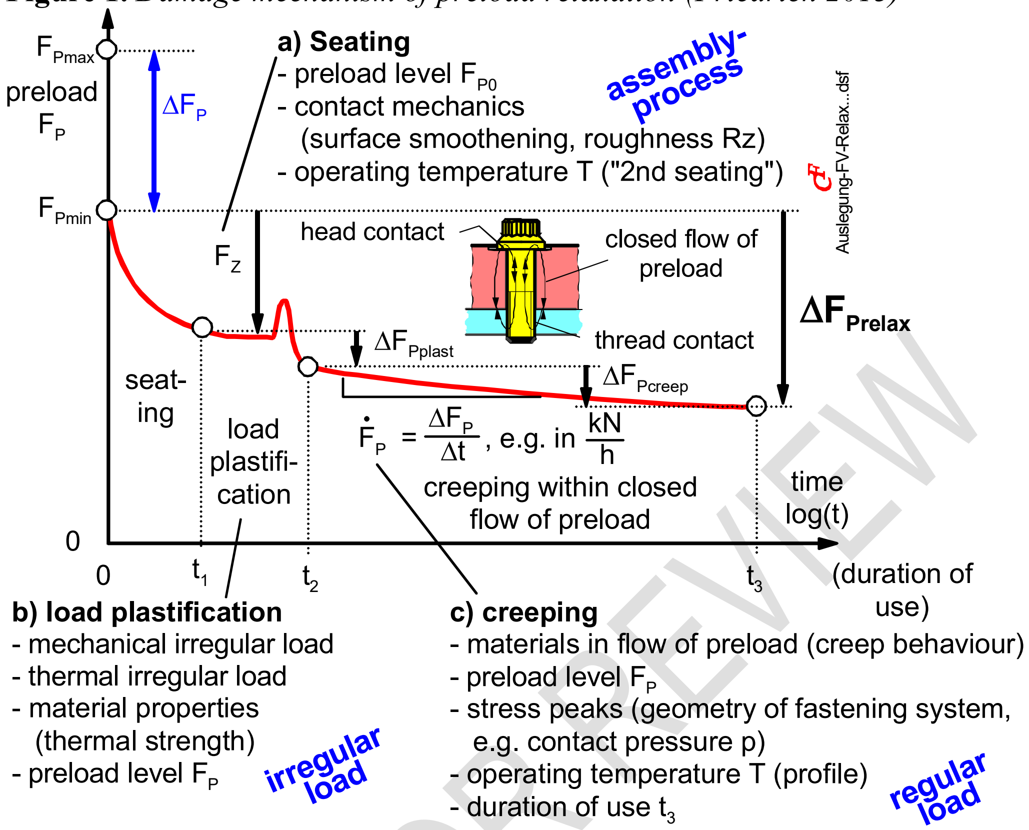

Literature Review

A comprehensive review of the existing literature (Peth 2022, Hubbertz 2020) shows that the preload relaxation behaviour in bolted joints, especially if lightweight configurations incorporating aluminium or magnesium components are used, depend on a complex interplay between thermal, mechanical and geometrical parameters. Early research focussed on the seating (e.g. Thum et al. (Thum 1940, Thum 1941) and self-loosening (e.g. Junker et al. (Junkers 1961, Junkers 1965)) of steel bolted joint connections. With steel-only components most of the relaxation will take place at the steel bolted joint as it is the component with the highest stress in the force flow. By the time lightweight applications became more and more common, the variety of material used in bolted joint connections increased accordingly. Lightweight materials like aluminium or magnesium are much more sensitive against temperature due to the lower melting point. Many publications (Chang et al. (Chang 2007), Chen et al. (Chen 1997), DeJack et al. (DeJack 2010), Jaglinski et al. (Jaglinski 2007)) tested the preload relaxation behaviour of aluminium diecasting alloys in real component systems, but due to different geometric specifications and limited variation parameters the results aren't comparable or transferrable to other systems. In addition, Scheiding (Scheiding 2001) investigated the usage characteristics of bolted joints containing magnesium components. Extensive series of experimental investigations were carried out in the doctoral thesis of Peth (Peth 2022). Influence factors like preload, temperature, clamping length, diameter of the clamped parts, thread engagement, roughness of the surface areas and materials (various aluminium alloys as well as steel clamped parts and nuts) were systematically investigated to also see their interdependences. The measurements were done by tactile displacement method and therefore only at discrete times. Also, analytical calculation methods were developed for example by Hubbertz (Hubbertz 2020) and Kempf (Kempf 2022), which provide good results for the evaluated test set-ups, but struggle with transferability to other component systems as shown in Kempf et al. (Kempf 2025). Therefore, a new calculation method is developed by Held (Held 2027) and will be released next year. Parts of the experimental work will be shown in this publication.

Methodology and experimental procedure

As described before only a sufficiently high preload level ensures the proper functionality of any bolted joint and will be reduced during operation because of the damage mechanism of preload relaxation. Unfortunately, we cannot measure the current preload directly, but there are several measurement methods from which the preload can be determined. The most common methods are shown in **Figure 2**. The easiest way is to use a load cell in the load path (as an additional clamped part) which allows a continuous measurement and isn't affected by bolt creep. Strain gauges inside the load cell can be calibrated with a reference force to determine the preload. Also, these load cells can be used over a long time with small signal drift. The problem is that the load cell changes the resilience of the bolted joint connection which leads to a different preload relaxation behaviour. Because every experiment needs a load cell, large-scale experiments over a long period of time are impractical. Additionally, these load cells cost around 1.500 €. Ultrasonic bolted joint connections, which measure the elongation of the bolt, are not suitable for a continuous measurement and will change their behaviour if bolt creep occurs. For large-scale experiments the tactile displacement measurement is the best option, as it is very cheap and the preparation of the specimen is not very time consuming or mechanically complex. The biggest problem is, that a continuous measurement is not possible and can only be done at controlled and stationary room temperature. Bolt creep can also only be seen if the bolted joint is disassembled. Details of the usage for preload measurement with tactile displacement method can be found in (Peth 2022). The best method to determine the preload precisely over time is to attach strain gauges to the bolt and continuously measure the change of resistance during the experiment.

All measurements of this paper are done with strain-gauge equipped bolts. The method is developed in (Held 2027, Held 2025) and has proven reliable under demanding exposure conditions such as elevated temperatures up to T ≤ 150 °C combined with high mechanical loads (assembly load $F_M = 35\ kN$).

Specialized strain gauges configured in a full Wheatstone bridge circuit (comprising four active gauges) to compensate for bending, temperature, and torsional influences on the bridge output signal. Each arrangement consists of two vertical and two horizontal strain gauges configured strictly to capture axial normal strain corresponding to the bolt load. These are hot-bonded onto the outer bolt shank below the head, as shown in **Figure 3**.

Figure 2. *Measurement methods to determine the preload; Picture of ultrasonic measurement method from Jenne et al. (Jenne 2015)*

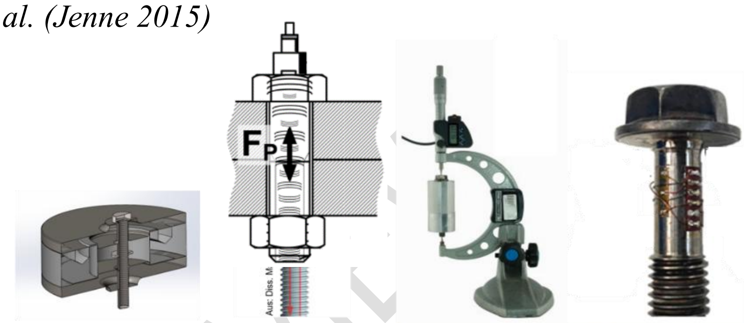

Criterion \ Measurement method	Load cell	Ultra Sonic	Tactile Displacement	Strain Gauge
Resilience change	☹	☺	☺	☺
Continuous measurement	☺	☹	☹	☺
Creep compensation of bolt	☺	☹	😐	☺
Time dependency of measurement	☺	☺	☺	😐
Large-scale experiments	☹	😐	☺	☹
Costs (money & effort)	😐	😐	☺	😐

Hexagon head bolts of nominal size M10x90 and property class 10.9 with full-length threading up to the bolt head were utilized. Because applying the strain gauges requires a uniform surface with low roughness, the thread directly below the head was turned down over a height of $h = 17\ mm$ to a diameter of $Ø7.8\ mm$. A vertical bore of $Ø1.8\ mm$ drilled through the bolt head onto the newly created surface provided lead wire access. Preliminary tests revealed that the signal, despite using the full-bridge configuration, contained a relevant thermal influence which adds to the strain-induced resistance change. The thermal-induced resistance change led to a distinct temperature drift on the order of several hundred Newtons, which was mechanically non-existent. The reason for that was an unbalanced bridge due to manufacturing inhomogeneities during manual application of the strain gauges such as non-uniform adhesive layer thickness, angular misalignment between individual strain gauges or intrinsic resistance tolerances of the gauges. Using an additional balancing resistor made of Balco nickel-iron alloy (Ni-Fe) in the Wheatstone bridge was identified as an effective countermeasure. Its core property is a strong resistance increase with rising temperatures, which has to be adjusted to compensate the bridge detuning and temperature induced effects. Figure 3 illustrates the integration of this component into the circuit (bottom left side) alongside its dampening effect on the unmounted bolt signal during thermal exposure (bottom right side). To show the difference between the regular full-bridge circuit with and without the balancing resistor, four bolts (two compensated against thermal drift, two uncompensated) were heated up to 150 °C in a controlled environment (heating rate: 1 °C/min) where the temperature was held for four hours and again cooled down to room temperature (cooling rate: 1 °C/min). The uncompensated bridge shows an apparent force F_{ap} of -900 N up to nearly -1400 N, whereas the compensated bridge is in the range of $F_{ap} = \pm 150\ N$, which mainly occur during temperature changes. Therefore, all measurements shown in this paper are done with individually compensated strain gauge bolts.

Figure 3. *Layout and connection diagram of the strain gauge bolted joints used in a full-bridge configuration, showing the resulting advantages and disadvantages (top), as well as the design and effect of the friction resistance implemented in the full-bridge circuit to compensate for temperature drift (bottom) (Held 2027)*

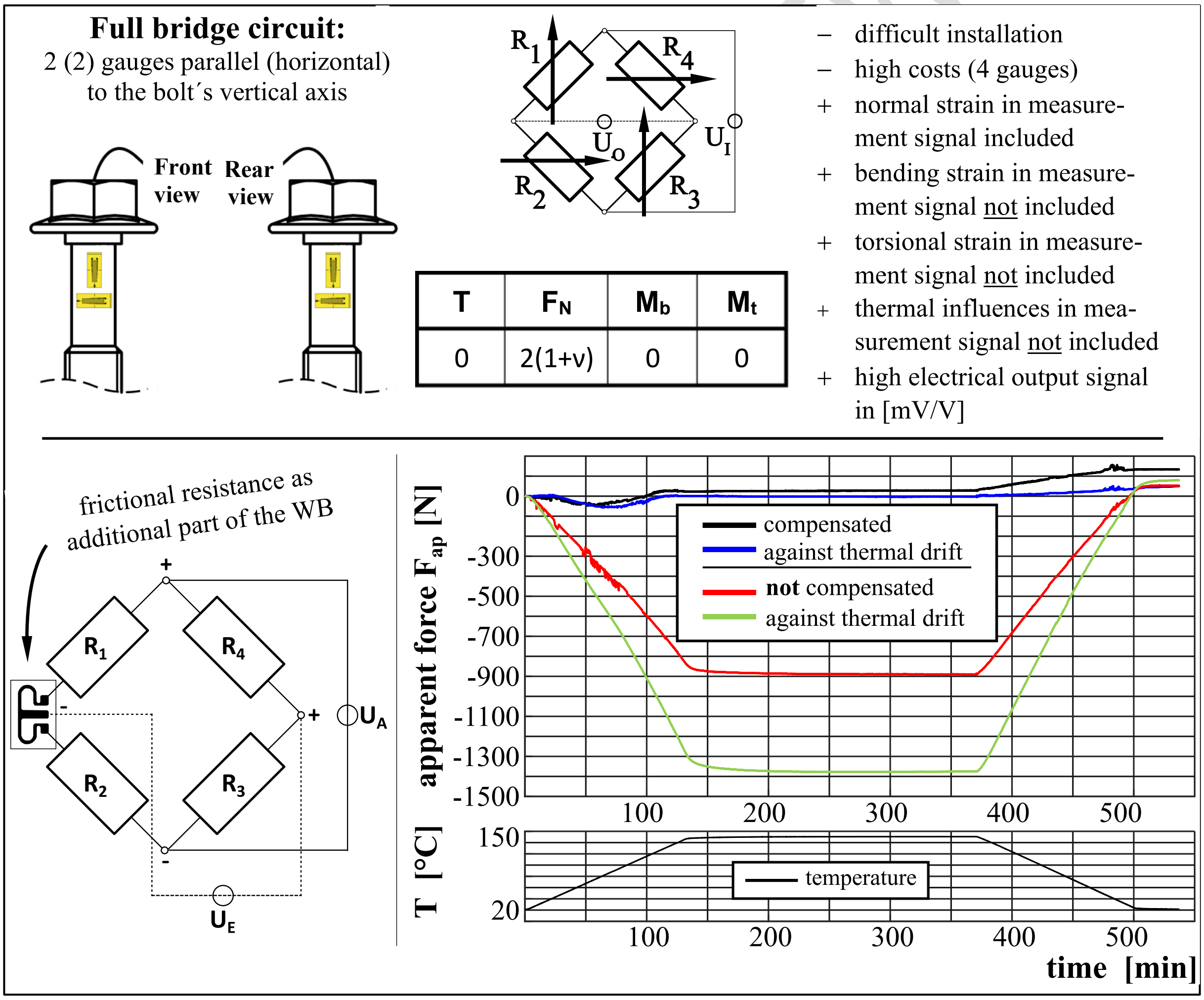

Literature review

For this paper only single-bolted cylindrical joints were investigated. Two types of bolts were used, both M10 steel bolts with property class of 10.9 having full-length threading and an external hexagon drive. They differ regarding the head bearing diameter, whereas the bolt similar to EN 1665 has a flange and therefore bigger head bearing diameter of roughly 19,6 mm and the ISO 4017 only has a head bearing diameter of roughly 14,6 mm. The material of all clamped parts and nut parts is a wrought aluminium alloy (EN AW-6082 T6511, 3.2315). The clamping length is $l_k = 2d$ (nominal diameter $d = 10\ mm$), the thread engagement varies between $m_e = 1{,}5d, 2d$ and $3d$. The outer diameter of the clamped part and nut part is always $D_A = 4d$. The contact areas between the bolt head and clamped part as well as the thread were lubricated with a high-temperature MoS_2-based paste. The bolted joints were tightened using a torque wrench applied to the bolt drive. Using real-time strain gauge signals, the initial preload was controlled precisely to target values of $F_M = 30\ kN, 35\ kN$ and $40\ kN$. Thermal exposure was conducted in a climate chamber capable of running defined temperature profiles. A relatively slow heating and cooling rate of $1\ °C/min$ was strictly maintained, while the temperature level before and after the exposure remained at $T_0 = 20\ °C$. The investigation focusses on the evaluation of the preload change during heating up to the exposure temperature T_1 as well as the preload relaxation behaviour as a function of design parameters like thread engagement, initial preload force and different head bearing diameters which will cause different stresses in the head contact area. In addition, its investigated, if retightening of the bolted joint connection can lower the overall preload loss.

Experimental results

General behaviour

Figure 4 shows a representative preload force curve obtained for a typically lightweight joint configuration. The system explained above, a steel bolt combined with a clamping part and nut made of aluminium, was investigated here in addition to the usage of the three thread engagement lengths m_e = 1.5d, 2d, and 30d and to initial preload levels F_{P0} = 30 kN and 35 kN. The bolt type was EN 1665, the tests were performed with an exposure temperature of T_1 = 150 °C. The specimens were heated from T_0 = 20 °C to T_1 = 150 °C, held at T_1 for t_1 = 100 h, and subsequently cooled back to T_0. For each test condition, the mean of three individual measurements is plotted together with the corresponding upper and lower deviations, which are indicated by shaded bands.

Figure 4. *Preload force of a lightweight bolted joint operated at T_1 = 150 °C as a function of the thread engagement m_e and the assembly preload level F_{P0}*

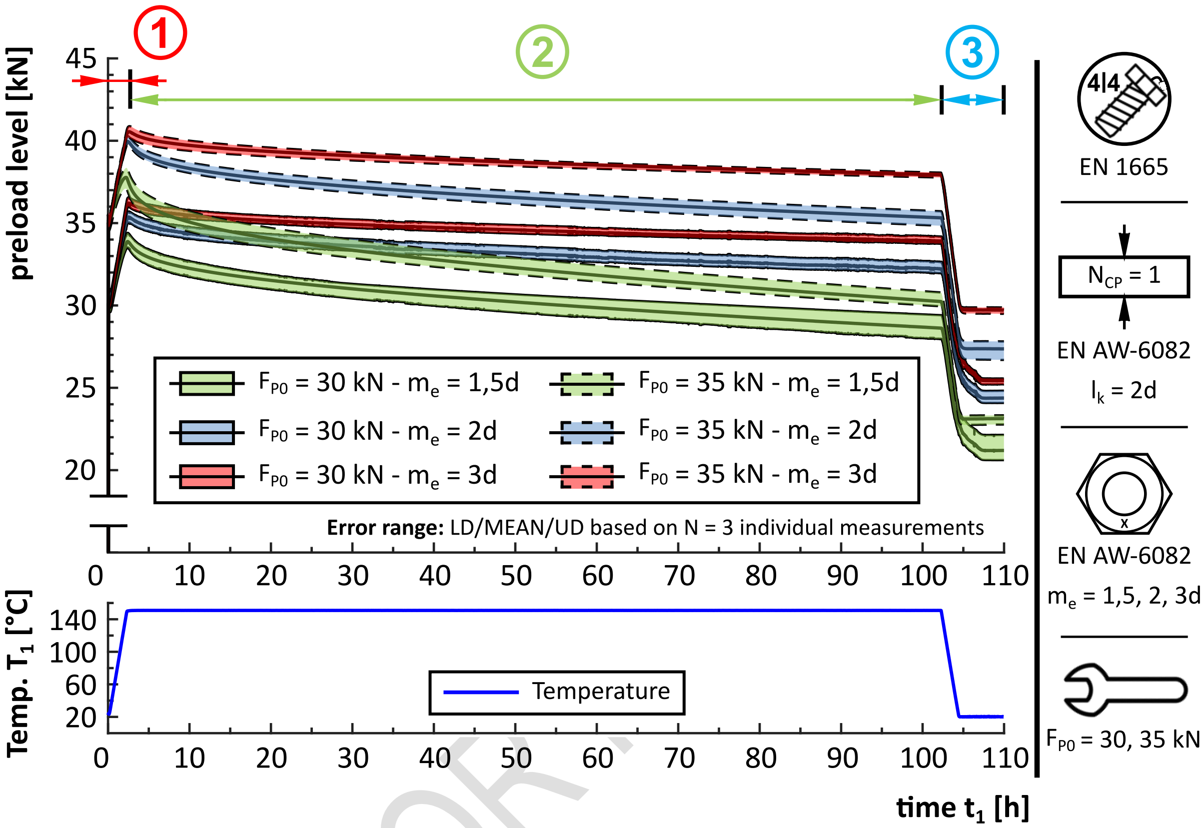

A key feature of the preload force curve shown above is that it closely reflects the actual behaviour of similar joint connections at elevated exposure temperatures over time very well. This requires the explained measurement technique specifically adapted to these conditions. The initial rise in the preload level (**Phase 1**) is clearly visible in each case; this is due to the different coefficients of thermal expansion of the steel-bolt and the clamping components made of aluminium. From there, all curves are shifting into a phase of continuous preload decline, which generally decreases with increasing exposure time (**Phase 2**). After finally reaching T_0 again, a permanent loss of preload $\Delta F_{VRelax} = F_{P0} - F_V$ (t_A = 100 h) becomes apparent, which constitutes the actual problem (**Phase 3**). This loss is visibly greater than the increase in preload force in Phase 1. Overall, there is a permanent loss of preload.

Extended influence of the preload

Figure 5 shows the extended influence of different assembly preload levels F_{P0} on the thermally induced increase in preload ΔF_{Vth} at the beginning of the test and on the subsequent preload relaxation process for a thread engagement length of m_e = 1.5d and an exposure temperature of T_1 = 150 °C. Initially, ΔF_{Vth}

shows an inverse relationship with the assembly preload, with the measured increase becoming smaller as the initial preload increases.

Figure 5. *Influence of the initial preload on the residual preload force at a thread engagement length of $m_e = 1.5d$ and a thermal load of $T_1 = 120$ °C*

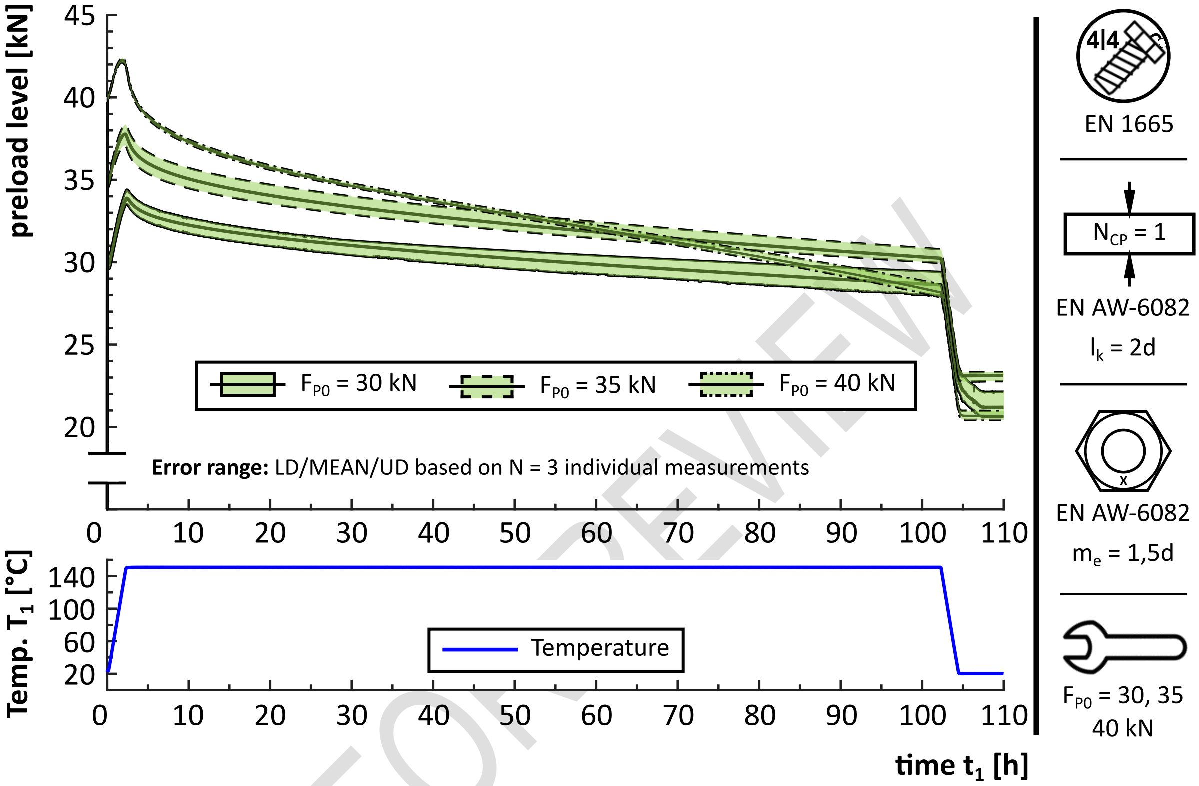

Values of approximately 4 kN, 3 kN, and 2 kN are obtained for F_{P0} = 30 kN, 35 kN and 40 kN, respectively. After completion of the heating phase, all curves are showing a pronounced decrease in preload. Considering only the 100 h exposure period at T_1, the largest decrease is observed for F_{P0} = 40 kN, with ΔF_V = -12 kN. This value considerably exceeds the decreases measured for F_{P0} = 35 kN (-4.5 kN) and F_{P0} = 30 kN (-1.5 kN). Consequently, by the end of the exposure period, the preload associated with the highest assembly preload is already slightly lower than that associated with the initially lowest assembly preload. For comparable lightweight joints, this indicates that the initial benefit of a higher assembly preload can be lost within a relatively short period due to the pronounced stress- and temperature-dependent preload relaxation. As a result, a higher initial preload may ultimately lead to a lower preload under operating conditions and thus directly compromise the functionality of the joint.

After cooling to room temperature again, the residual preload values for F_{P0} = 40 kN and F_{P0} = 30 kN are nearly identical, amounting to 20.7 and 21.2 kN, respectively. Thus, the specimen initially preloaded to F_{P0} = 30 kN retains approximately 0.5 kN more preload than initially preloaded to F_{P0} = 40 kN. In contrast, an assembly preload of F_{P0} = 35 kN results in the highest residual preload of 23.1 kN, approximately 2 kN above the other two configurations. These results demonstrate that high utilization of the joint components through increased assembly preload, although generally desirable, can result in substantially different in-service behaviour in comparable lightweight joints. Due to the associated preload relaxation, this behaviour can compromise the overall function of the joint within a relatively short period of time.

Influence of the head bearing geometry

Figure 6 shows the influence of the bearing geometry under the bolt head on the preload behaviour. The flange-head geometry used in the previous experiments (EN 1665, bearing diameter $d_w \approx 19.6$ mm) is compared with a conventional hexagon-head geometry (ISO 4017, $d_w \approx 14.6$ mm) for thread engagement lengths of me = 1.5d, 2d and 3d. The aim is to determine whether the 66 % smaller bearing area (for a hole diameter of $d_h = 11$ mm) and the resulting higher bearing pressure led to a significant deviation from the behaviour previously observed for the flange-head bolts.

A notable initial observation is the substantially lower thermally induced increase in preload ΔF_{Vth} for the hexagon-head bolts. Irrespective of the thread engagement length, ΔF_{Vth} remains comparatively low at approximately 4-5 %. In contrast, the flange-head bolts are showing considerably greater differences between the individual thread engagement lengths, with increases of 11 %, 13 %, and 16 % for me = 1.5d, 2d and 3d, corresponding to values approximately two to three times higher than those obtained for the hexagon-head bolts.

Furthermore, the preload curves of the hexagon-head bolts are much more closely spaced and exhibit similar rates of decrease. This indicates that the dominant mechanism responsible for preload loss shifts from the engaged thread region toward the bearing area under the bolt head. After final cooling to T_0, the residual preload forces of the hexagon-head bolt configurations are also similar, and the previously observed benefit of a greater thread engagement length (cf. Figure 4) is no longer apparent. In contrast, the larger flange bearing area results in distinct preload loss rates during exposure at elevated temperature depending on m_e. After removal of the thermal load, these differences result in clearly distinguishable residual preload levels.

Figure 6. *Influence of the head bearing geometry (EN 1665, ISO 4017) on the residual preload force as a function of the thread engagement at a thermal load of T_1 = 120 °C*

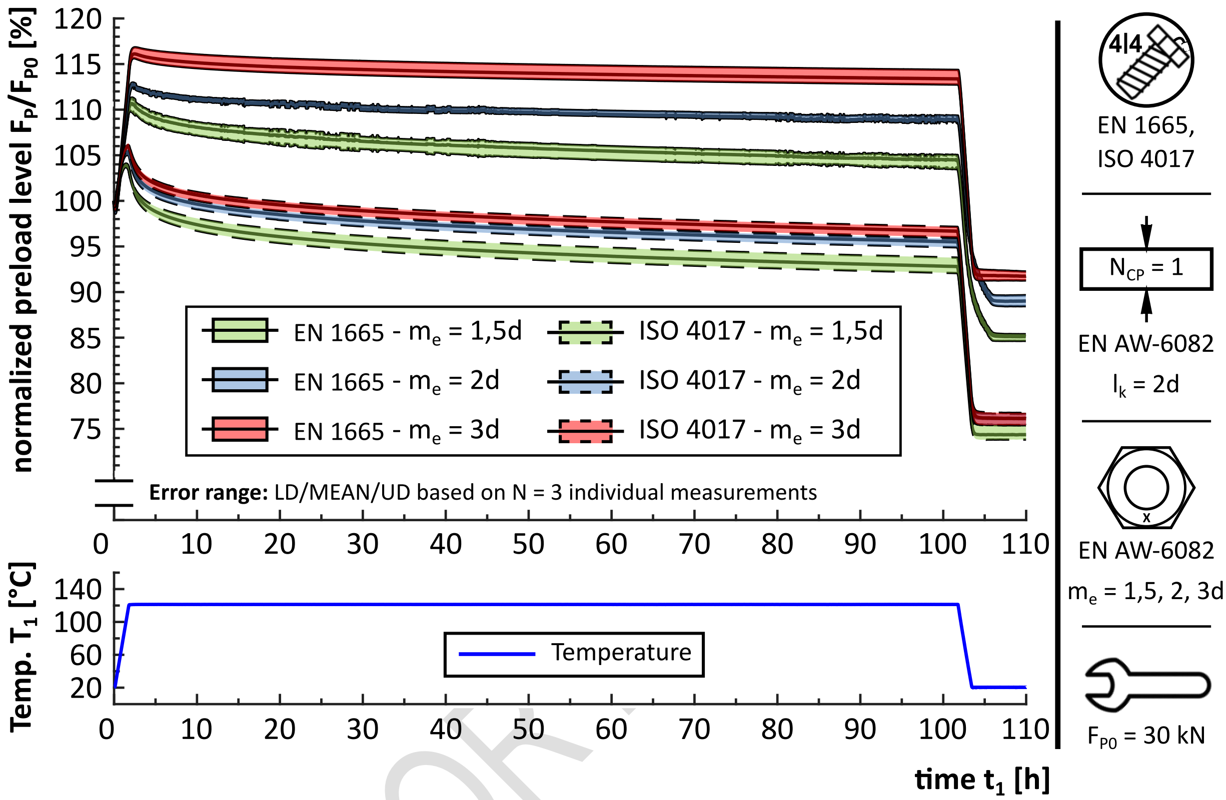

Figure 7 additionally compares the experimentally determined values of the thermally induced preload increase ΔF_{Vth} for both bolt geometries with the value calculated according to VDI 2230 (green bar). The calculation specified in VDI 2230 does not account for geometric parameters such as thread engagement length or the bearing geometry under the bolt head. The time t_{max} at which the maximum preload force is reached is indicated also.

It is initially apparent that, for the EN 1665 bolts, the maximum preload is reached after completion of the actual heating period of t_{heat} = 100 min (ΔT = 100 °C at a heating rate of 1 °C/min) in all test configurations. In contrast, the ISO 4017 bolts show the opposite behaviour, with only the test at m_e = 3d reaching its maximum preload at a time corresponding to t_{heat}.

The thermally induced preload increases ΔF_{Vth} calculated according to VDI 2230 is, on average, reached by only one of the investigated test configurations (EN 1665 at m_e = 3d). All other results obtained with EN 1665 bolts remain moderately below the calculated value, whereas substantially lower values are observed for the ISO 4017 bolts. This indicates that plastic deformation of the lightweight joint components - primarily within the clamped component and at the nut thread contact and, to a lesser extent, within the bolt (cf. Peth 2022), can already occur to such an extent during heating that any further increase in preload is getting limited despite the continuously increasing temperature. The extent of this plastic deformation depends on both the bolt-head geometry and the thread engagement length in the nut.

For ISO 4017 bolts, the difference between m_e = 1.5d and 3d is approximately 15 % and thus less than half the corresponding difference observed for EN 1665 bolts (approximately 35 %). The substantially lower dependence on thread engagement length for ISO 4017 supports the hypothesis discussed above that, due to the smaller bearing area of this bolt type, a major portion of the plastic deformation occurs at the surface of the clamped component beneath the bolt head.

Figure 7. *Comparison of the thermally induced preload change ΔF_{Vth} for ISO 4017 and EN 1665 bolted joint geometries at thread engagements m_e = 1.5d, 2d and 3d with the value calcu-lated in accordance to VDI 2230*

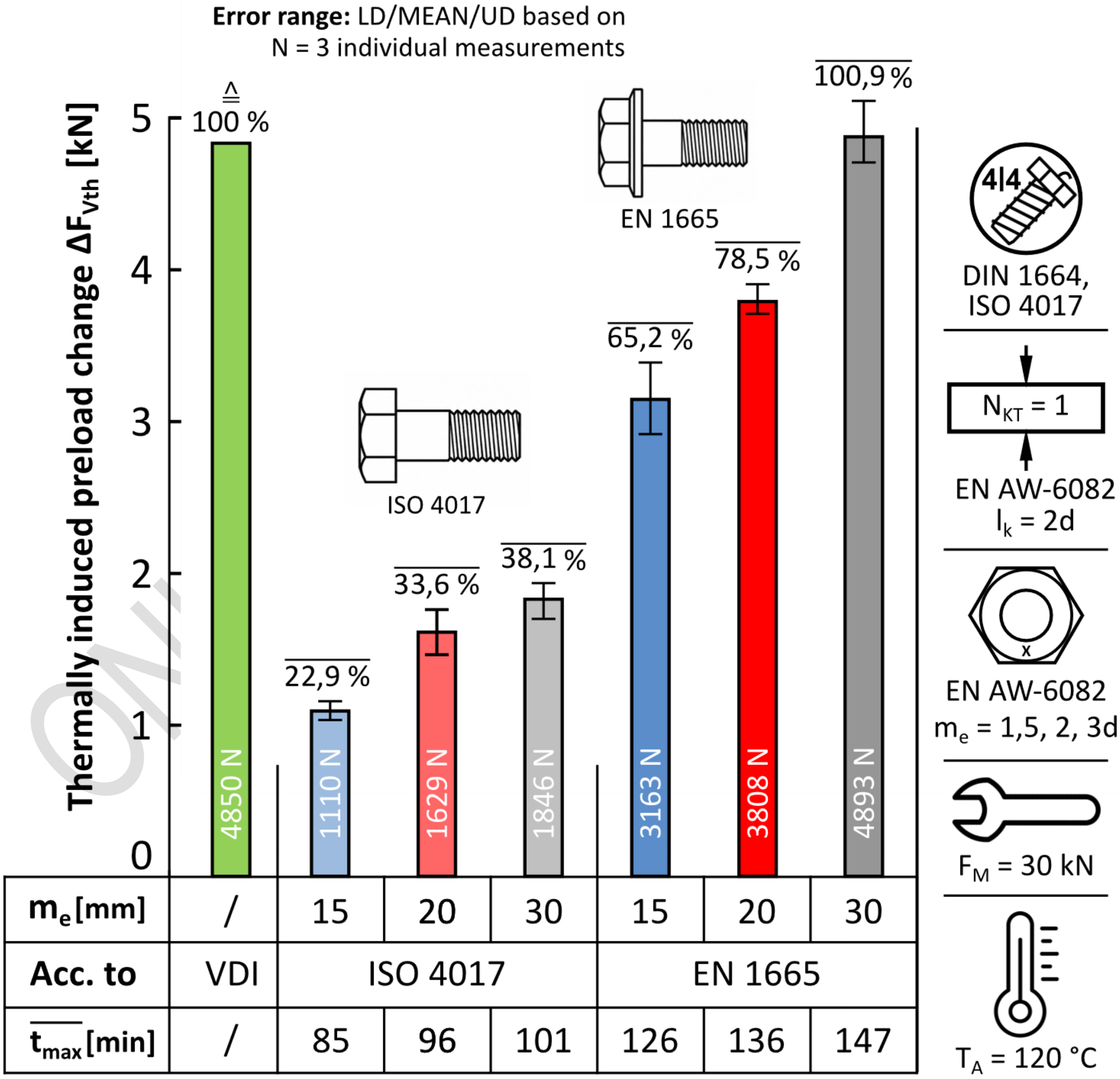

Figure 8 shows comparative surface profile measurements, restricted to the region relevant to the present analysis. The profiles extend from the unloaded surface and the onset of the contact region on the left to the transition into the chamfered drilling hole on the right, which is indicated by the steep drop in the profile curves.

On the left side of both profiles, the unloaded regions of the specimen surfaces are clearly visible, showing the slight waviness resulting from the machining process during production. The blue profile (EN 1665) begins to deviate from this characteristic surface pattern earlier, which can be attributed to the larger bearing area of the flange-head bolt. This is followed by a slight but continuous decrease towards the clearance hole at an approximately constant rate. The observed profile corresponds well to the internally bearing geometry of the bolt, with a maximum plastic deformation of approximately 15 µm.

Figure 8. *Plastification of the clamping surface on the head side depending on the screw head geometry for a thread engagement* $m_e = 3d$

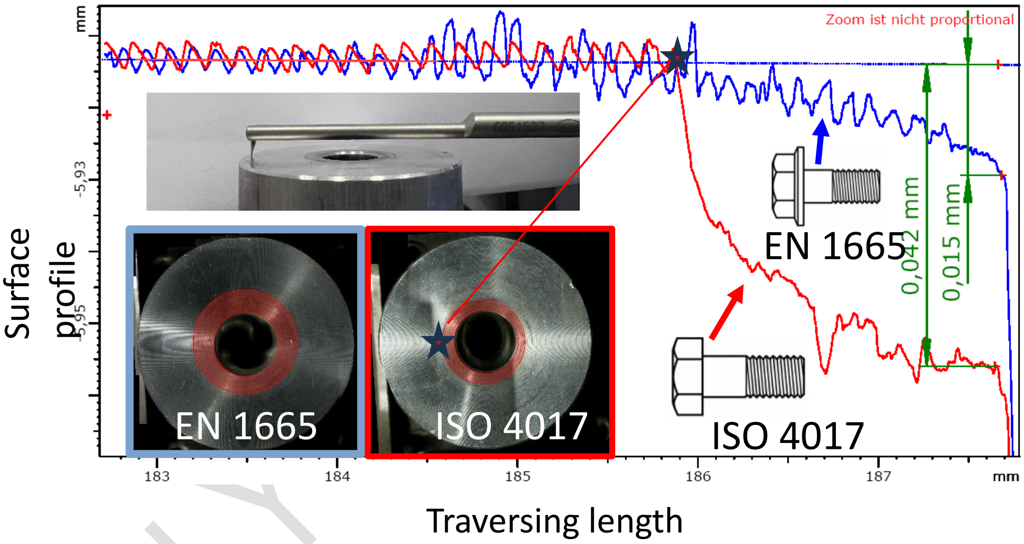

In contrast, the red profile (ISO 4017) follows the unloaded surface pattern over a longer distance before showing a sudden and strong drop, indicating substantial local plastic deformation. Its maximum value reaches approximately 42 µm and is therefore almost three times more than measured for the EN 1665 configuration (approximately 15 µm). This result confirms the hypothesis that the smaller bearing area of the ISO 4017 bolt leads to substantially greater plastic deformation of the clamped component beneath the bolt head.

Impact of repeated tightening processes

Figure 9 shows the influence of repeated retightening to F_{P0} after defined exposure periods for thread engagement lengths of $m_e = 1.5d$ and 2d. After initial tightening to F_{P0}, the joints were exposed to $T_1 = 120$ °C for $t_1 = 50$ h and subsequently cooled back to T_0. Before the end of a holding time of approximately

1 h, the joints were retightened to F_{P0}. This procedure was repeated five times, resulting in a total exposure time of t_{total} = 250 h.

The previously observed effect that the initial thermally induced increase in preload ΔF_{Vth} decreases with increasing thread engagement length is also evident in these tests. This behaviour results from plastic deformation occurring simultaneously in the nut thread region, which limits the thermally induced increase in preload. During the first hours of exposure, the preload loss amounts to approximately 5 % for m_e = 1.5d and is therefore slightly but noticeably higher than the approximately 3 % observed for m_e = 2d.

With an increasing number of retightening cycles, however, the behaviour of the two configurations becomes progressively more similar, as the difference in ΔF_{Vth} decreases with each heating cycle. This indicates that the plastic deformation described above occurs predominantly during the initial cycle. Although the preload relaxation rate under thermal exposure remains higher for m_e = 1.5d than for m_e = 2d even during the final cycles, the absolute preload losses decrease progressively. In the last cycle, the losses amount to approximately 1 % for m_e = 2d and 2 % for m_e = 1.5d.

Figure 9. *Effect of repeated retightening operations on the residual preload force as a function of the thread engagement at an exposure temperature of T_A = 120 °C*

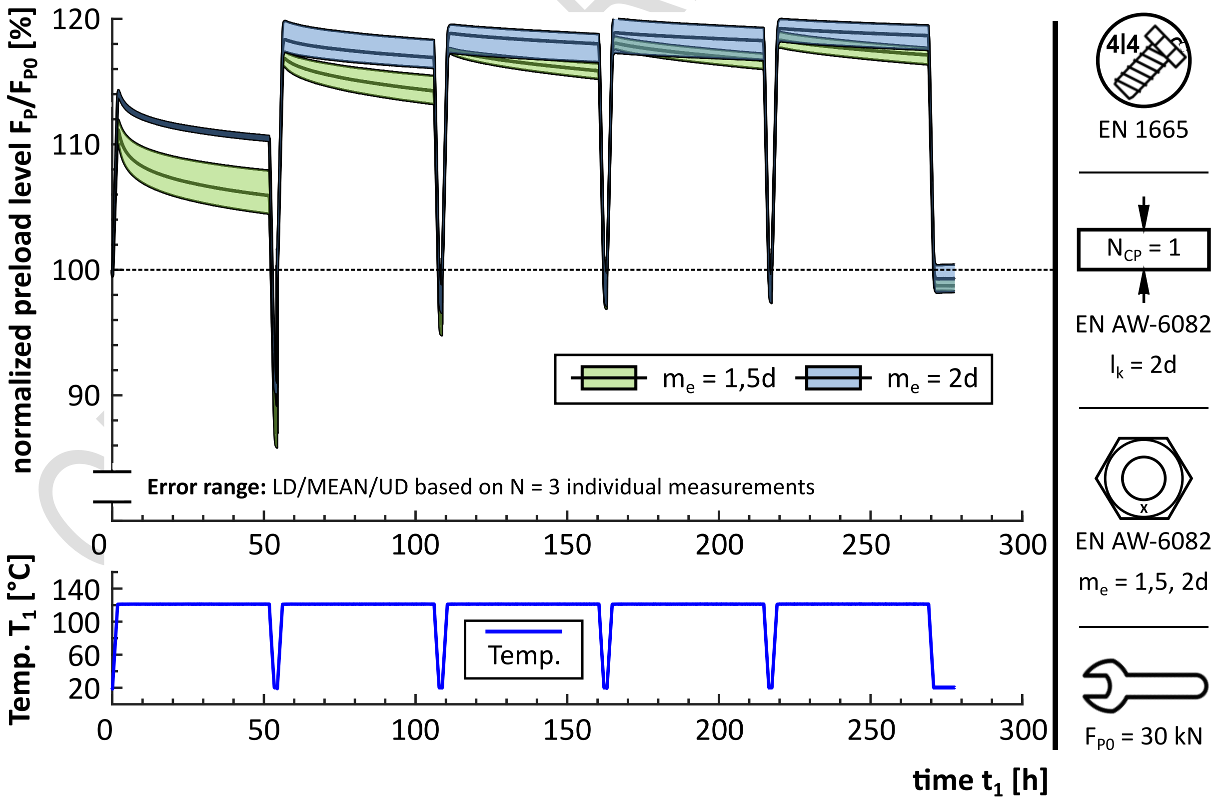

The results therefore show that retightening the joint to its initial preload after thermal exposure has a beneficial effect on subsequent preload relaxation behaviour. Considering the additional effort involved relative to the resulting benefit, one or two retightening operations appear to be sufficient.

Summary and conclusion

The experimental investigations in this publication demonstrate that preload relaxation leads to significant losses during thermal exposure, which must already be considered during the design process. It is shown that joint design according to VDI 2230 guideline is insufficient if lightweight materials are exposed to elevated temperatures. The standard should be expanded to include factors that have high impact on the preload relaxation.

Furthermore, the degradation of lightweight material properties at elevated temperatures necessitates a re-evaluation of the recommended assembly preload level. High initial preloads induce severe relaxation losses and become particularly critical at reduced thread engagement lengths. For instance, joints assembled with an initial preload of F_{P0} = 40 kN exhibited a lower residual preload at the end of the test duration than those tightened to F_{P0} = 30 kN. Reducing the thread engagement length resulted in preload losses of approximately 5 % to 15 %, even under low additional thermal forces and moderate exposure temperatures of 120 °C. It was also demonstrated that altering the bolt head bearing area fundamentally changes the systems behaviour. With less head bearing surface the influence of a reduced thread engagement cannot be seen anymore. In tactile profilometry (standardized stylus measurements) we could see the higher plastification in the contact area for the bolted joint with smaller bearing surface area. This geometry change leads to a shift where preload relaxation took place. Retightening the joint after the initial cycle proved to be an effective mitigating measure. The localized deformation, strain hardening and surface smoothening that occur during the first heating cycle effectively reduced the preload loss in the following thermal cycles.

The huge amount of influence factors of preload relaxation makes it hard to find an easy way to estimate the preload loss of a specific bolted joint connection. The measurement method which is used in this paper gives good hints about the point of time when the preload loss happens. The rate of preload relaxation, which can be seen best with direct measurement methods, gives a good estimation of the influence of design changes. With all gained experiment data, an easy-to-use calculation method could be developed to estimate the preload loss. This will be the objective of future research work.

References

(Arz 2003) Arz, U., Berger, C., Kaiser, B. u. Kremer, U.: Grenzflächenpressung von Leichtmetallen unter kontinuierlicher Beanspruchung bei Temperaturen bis 150 °C. Konstruktion 55 (2003) 3, S. 63-67.

(Ba-Saleem 1991) Ba-Saleem, M. O.: Theroretische und experimentelle Untersuchungen der Setz-verluste an Schraubenverbindungen, Technische Universität Chemnitz, Dissertation. Chemnitz, 1991.

(Chang 2007) Chang, C.-C. u. Wang, Q. G.: Modeling of Bolt Joint Behavior of Cast Aluminium Alloy (A380-T5) by Coupling Creep and Pasticity in Finite Element Analysis. Metallurgical and Materials Transactions / B, Process metallurgy and materials processing science 38B (2007) 4, S. 607-613.

(Chen 1997) Chen, F. C., Jones, J. W., McGinn, T. A., Kearns, J. E., Nielsen, A. J. u. Allison, J. E.: Bolt-Load Retention and Creep of Die-Cast Magnesium Alloys (1997), S. 13-22.

(DeJack 2010) DeJack, M. A., Ma, Y. u. Craig, R.: Bolt Load Relaxation and Fatigue Prediction in Threads with Consideration of Creep Behavior for Die Cast Aluminum. SAE Technical Paper 2010-01-0965 (2010), S. 29–38.

(Duchard 2013) Duchardt, M.: Bewertung des Vorspannkraftverlustes in Schraubenverbindungen unter kombinierter mechanischer und thermischer Beanspruchung. Zugl.: Darmstadt, Techn. Univ., Dissertation, 2013. Berichte aus der Werkstofftechnik, Bd. 2013, 2. Aachen: Shaker 2013.

(Friedrich 2013) Friedrich, C., Hubbertz, H.: Relaxation of clamp force in fastened carbon composite structures with thermal load. International Conference on Composites Engineering ICCE-21, Santa Cruz de Tenerife, 2013.

(Held 25) Held, T., Peth, J. Reliable continuous force measurements at ambient and elevated temperatures with strain gauges using the example of bolted joints, 8th International Conference on Integrity, Reliability, Failure, Porto/Pt, 2025.

(Held 2027) Held, T.: Dissertation University of Siegen, in progress, approx. 2027.

(Hubbertz 2020) Hubbertz, H.: Beitrag zur Auslegungsrechnung von Leichtbauschraubenverbindungen im Hinblick auf die Vorspannkraftrelaxation. Siegen: universi - Universitätsverlag Siegen 2020.

(Jaglinski 2007) Jaglinski, T., Nimityongskul, A., Schmitz, R. u. Lakes, R. S.: Study of Bolt Load Loss in Bolted Aluminum Joints. Journal of Engineering Materials and Technology 129 (2007) 1, S. 48-54.

(Jenne 2015) Jenne, M., Hubbertz, H., Friedrich, C., Bär, C.: Improved mechanical preload measurement of bolted joints for light weight design with CFRP components. 2015 ASME International mechanical engineering Congress and Exposition, Houston, Texas, 2015.

(Junker 1961) Junker, G.: Sicherung von Schraubenverbindungen durch Erhaltung der Vorspannung. In: Draht-Welt 47. Jg., S. 936-943, 1961.

(Junker 1965) Junker G, Blume D: Neue Wege einer systematischen Schraubenberechnung. Düsseldorf: Michael Triltsch Verlag, 1965.

(Kempf 2022) Kempf, A.: Bewertung der zeit- und temperaturabhängigen Vorspannkraftrelaxation in Schraubenverbindungen. Schriftenreihe des Zentrums für Konstruktionswerkstoffe (MPA + IfW): "Werkstofftechnologie". Shaker Verlag, Düren, Oktober 2022.

(Kempf 2025) Kempf, A., Peth, J., Hubbertz, H.: Rechnerischer Ansatz zur Prognose des Vorspannkraftverlusts durch Relaxation. 8. VDI-Fachtagung Schraubenverbindungen, 12. und 13.11.2025, Leipzig.

(Peth 2022) Peth, J.: Einflüsse auf das Vorspannkraftrelaxationsverhalten von Schraubenverbindungen im Leichtbau, Siegen: Universi, 2022.

(Scheiding 2001) Scheiding, W.: Beitrag zur Ermittlung der Gebrauchseigenschaften von Schraubenverbindungen mit Magnesiumkomponenten. Darmstadt: Shaker, 2001.

(Thum 1940) Thum A, Würges M: Die zweckmäßige Vorspannung in Schraubenverbindungen. Deutsche Kraftfahrtforschung, Heft 43. VDI-Verlag, 1940.

(Thum 1941) Thum A, Lorenz H: Vorspannung und Dauerhaltbarkeit an Schraubenverbindungen mit einer oder mehreren Schrauben. Deutsche Kraftfahrtforschung, Heft 56. VDI-Verlag, 1941.

VDI Richtlinie 2230-1:2015-11. Systematische Berechnung hochbeanspruchter Schraubenverbindungen. Blatt 1: Zylindrische Einschraubenverbindungen.